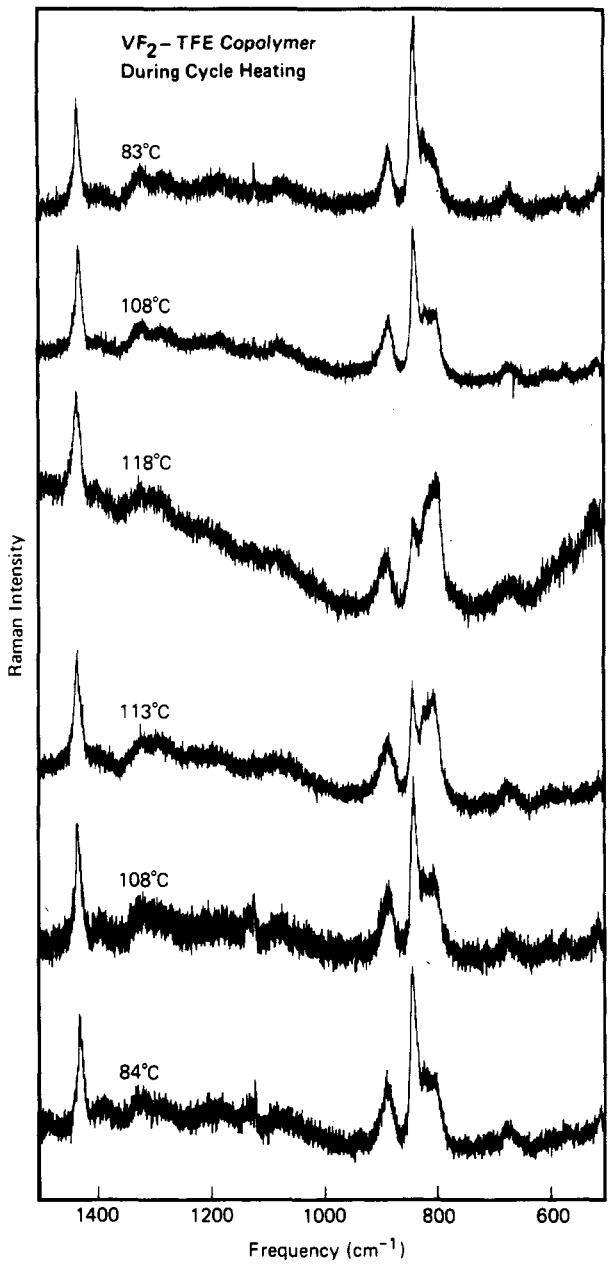

Figure 2. Raman spectra of VF_2/TFE copolymer as a function of temperature. (excitation wavelength = 488.0 nm, resolution = 4 cm^{-1}).

The feasibility of using Raman measurements to determine Curie behavior in VF_2 copolymers has been demonstrated. The characterization of these order–disorder transitions by nondestructive spectroscopic methods will be of extreme importance in studying VF_2/TFE copolymers with VF_2 compositions[15] less than 50%. In these cases the Curie point will occur below room temperature and will not be easily accessible by conventional X-ray diffraction methods.

Acknowledgment. We acknowledge partial support for this work from the NSF Division of Materials Research under Industry/University Cooperative Research Grant DMR-8419095.

Registry No. Kynar 7201, 25684-76-8.

References and Notes

(1) Yagi, T.; Tatemoto, M.; Sako, J. *Polym. J. (Tokyo)* **1980**, *12*, 209.
(2) Furukawa, T.; Johnson, G. E.; Bair, H. E.; Tajitsu, Y.; Chiba, A.; Fukada, E. *Ferroelectrics* **1981**, *32*, 61.
(3) Yamada, T.; Ueda, T.; Kitayama, T. *J. Appl. Phys.* **1981**, *52*, 948.
(4) Tashiro, K.; Takano, K.; Kobayashi, M.; Chatani, Y.; Tadokoro, H. *Polymer* **1981**, *22*, 1312.
(5) Lovinger, A. J.; Davis, G. T.; Furukawa, T.; Broadhurst, M. G. *Macromolecules* **1982**, *15*, 323.
(6) Green, J. S.; Rabe, J. P.; Rabolt, J. F. *Macromolecules* **1986**, *19*, 1725.
(7) Lovinger, A. J. *Macromolecules* **1983**, *16*, 1529.
(8) Lovinger, A. J.; Johnson, G. E.; Bair, H. E.; Anderson, E. W. *J. Appl. Phys.* **1984**, *56*, 2412.
(9) Leonard, C.; Halary, J. L.; Monnerie, L.; Micheron, F. *Polym. Bull. (Berlin)* **1984**, *11*, 195.
(10) Hicks, J. C.; Jones, T. E.; Logan, J. C. *J. Appl. Phys.* **1978**, *49*, 6092.
(11) Koizumi, N.; Hagino, J.; Murata, Y. *Ferroelectrics* **1981**, *32*, 141.
(12) Tasaka, S.; Miyata, S. *J. Appl. Phys.* **1985**, *57*, 906.
(13) Lovinger, A. J.; Davis, D. D.; Cais, R. E.; Kometani, J. M. *Macromolecules* **1986**, *19*, 1491.
(14) Murata, Y.; Koizumi, N. *Polym. J. (Tokyo)* **1985**, *17*, 1071.
(15) Lovinger, A. J.; Cais, R. E.; Bair, H. E.; Johnson, G. E.; Davis, D. D.; Kometani, J. M.; Anderson, E. W. *Bull. Am. Phys. Soc.* **1986**, *31*, 611.

Jennifer Green and J. F. Rabolt*
IBM Almaden Research Center
San Jose, California 95120
Received October 14, 1986

Direct Measurement of Propagating Radical Concentration in a Semicontinuous Emulsion Polymerization

Achievement of a better fundamental understanding of free radical emulsion polymerization requires knowledge of the nature and concentration of the propagating free radical species. Direct observation of propagating free radicals in an emulsion polymerization had not been reported until the recent work of Ballard et al.,[1,2] who applied modern ESR techniques to observe propagating free radicals in a batch emulsion polymerization of methyl methacrylate. We have extended ESR analysis to semicontinuous acrylic emulsion polymerization and have studied the propagating free radical species as a function of polymerization temperature and particle size.

Semicontinuous emulsion polymerization, in which monomer is continuously added over several hours, is commonly used for the commercial preparation of latex polymers. This method is preferred primarily because it allows easy control of the polymerization temperature and the preparation of uniform copolymer compositions. Under suitable conditions the rate of polymerization is governed by the monomer feed rate. If it is assumed that monomer diffusion is not a rate-limiting process and that the bulk of the polymerization occurs isotropically within the latex particles, then in a semicontinuous system that has reached steady state the polymerization kinetics can be represented by eq 1, where [M] and [R•] represent the

$$\text{rate of monomer feed} = \text{rate of polymerization} = k_p[M][R^\bullet] \quad (1)$$

steady-state monomer and radical concentrations in the latex particles and k_p is the propagation rate constant. The validity of this equation has not been previously tested by independently measuring each term. The rate of monomer feed and the steady-state monomer concentration can be measured experimentally, and k_p can be estimated from analogous homogeneous polymerizations. The ESR measurements reported here now give us the steady-state radical concentration data which show that eq 1 is valid

0024-9297/87/2220-0457$01.50/0

Table I
Parameters for Semicontinuous Acrylic Emulsion Polymerization[a]

polym temp, °C	particle size,[b] nm	feed rate, 10^{-3} mol dm^{-3} s^{-1}	conversion, %	[R•], 10^{-5} mol dm^{-3}	[M], mol dm^{-3}	k_p,[c] dm^3 s^{-1} mol^{-1}	$\bar{n}$[d]
50	50	1.1	97	1.8	0.37	170	0.7
	500	1.2	95	5.5	0.62	35	2100
55	50	1.1	98	2.0	0.24	230	0.8
	500	1.2	94	4.5	0.69	39	1800
60	50	1.1	98	0.88	0.27	460	0.4
	500	1.2	94	1.8	0.68	98	710
65	50	1.1	98	0.61	0.27	670	0.2
	500	1.2	95	0.60	0.52	380	240

[a] Emulsion composition of 8 BA/91 MMA/1 MAA with 0.42 mequiv of $Na_2S_2O_8$ and of $NaHSO_3$ (based on monomer) added uniformly over about 180 min to a final total solids content of ~30%. All values obtained over the last 15% of monomer feed and expressed in terms of dm^3 of organic phase. [b] Approximate particle diameter determined by photon correlation spectroscopy. [c] Calculated from eq 1. [d] $\bar{n}$ is the average number of radicals per particle.

for a typical semicontinuous emulsion polymerization.

A composition of 8 parts (by weight) of butyl acrylate, 91 parts of methyl methacrylate, and 1 part of methacrylic acid was polymerized at four temperatures between 50 and 65 °C and at two very different particle diameters, ~50 and ~500 nm. Particle size was controlled by the initial surfactant level in the case of the 50-nm latices and by a low level of seed latex for the 500-nm latices. Polymerization was initiated by a redox couple of sodium persulfate and sodium bisulfite added uniformly with the monomer. Details of eight different polymerizations along with the observed steady-state monomer and radical concentrations for each are summarized in Table I. The steady-state monomer concentrations were obtained from small aliquots of the latex, which were analyzed by a standardized gas chromatography method.

For the determination of the steady-state radical concentrations, latex samples were removed from the reaction vessel under a nitrogen atmosphere, placed into an ESR sample tube at ambient temperature, rapidly frozen to −78 °C, and sealed under vacuum. The ESR spectra, obtained at −80 °C by computerized signal averaging on an IBM Instruments ER/200D spectrometer, all showed a propagating MMA terminal radical. A spectrum of a 500-nm particle size latex sample is shown in Figure 1. Radical concentrations were calculated by double integration of the signal and comparison to standards containing known concentrations of 2,2-diphenyl-1-picrylhydrazyl in benzene. The radical concentrations determined in this manner are estimated to have an error of less than ±50%.

Our standard sampling technique requires about 15 s for the transfer from reactor to cooling bath. In order to test the validity of our sampling technique, at each polymerization temperature a series of samples was collected with delay times varying from 15 to 60 s between sampling and freezing. No significant changes in the ESR signal intensities as a function of delay time were observed for polymerization temperatures between 50 and 65 °C. Samples obtained by our quick-freezing technique were stored for months at −78 °C without appreciable loss of signal intensity. At ambient temperature there is a slow loss of signal. At temperatures near the glass transition temperature of the polymer (~85 °C) the signal decays rapidly by a second-order process. Above 70 °C significant loss of radical signal is observed on the time scale of sampling; thus systems having lower glass transition temperatures or made at higher polymerization temperatures cannot be investigated without employing a more rapid freezing procedure.

Assuming that eq 1 is valid, values of k_p were calculated from the experimental feed rate and the observed steady-state monomer and radical concentrations that are shown in Table I. The calculated k_p values show an unexpected dependence on particle size. The k_p values calculated for the 50-nm latex polymerizations agree well with previously reported values of k_p for methyl methacrylate.[3-7] Thus for the small particle size latices under our specified conditions, eq 1 gives a valid representation of the polymerization.

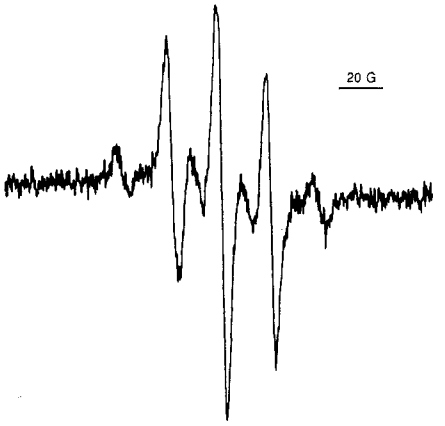

Figure 1. ESR spectrum (sum of 25 scans taken at −80 °C) of a sample taken from the semicontinuous emulsion polymerization at 55 °C of a monomer composition 8 BA/91 MMA/1 MAA. Final particle size was 500 nm.

The k_p values calculated for the 500-nm latex polymerizations are uniformly lower. This difference reflects the slightly higher radical concentrations observed in these systems relative to the analogous smaller particle size systems. We speculate that this difference is due to a modest inhomogeneity in the locus of polymerization in the larger latex particles. In the 500-nm glassy polymer matrix we hypothesize that monomer diffusion becomes a factor, and a significant concentration gradient is established with decreasing monomer concentration toward the particle centers. Due to higher conversion at the particle centers, the radical concentration is expected to exhibit an opposite gradient with increasing concentration toward the particle centers. The overall effect is a measurably higher steady-state radical concentration in the larger particle size latices. It is interesting to note that the difference in radical concentrations between the large- and small-particle latices decreases with increasing temperature; this trend is consistent with increased monomer diffusion with increasing temperature, resulting in a more homogeneous polymerization.

An Arrhenius plot for the 50-nm particle size polymerization rate constant data is linear; a similar plot for the rate constants from the 500-nm polymerization is less linear (see Figure 2). This behavior is consistent with our hypothesis of inhomogeneous polymerization in the larger particle size latices since the calculated k_p values would

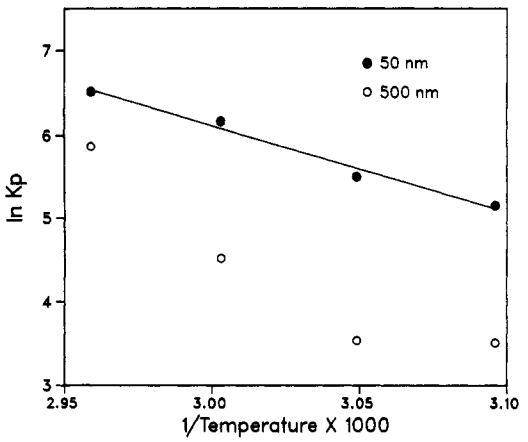

Figure 2. Arrhenius plot of propagation rate constants for small and large particle size latices. Data taken from Table I.

contain contributions from both monomer diffusion and propagation. The activation energy calculated for the propagation reaction for the 50-nm particle size data is 20 kcal/mol. This number is markedly larger than the value observed for radical propagation reactions in solution.[8] Presumably this larger value is a result of the very high viscosities present in the particles under conditions of high conversion.

Recent results reported by Ballard et al.[2] for batch emulsion polymerization of methyl methacrylate may be compared to the results obtained in this study. Although Ballard et al. did not report final particle size, we have inferred from their data that it was about 160 nm, intermediate to the two particles sizes examined in this study. Allowing for the minor compositional difference, their values of $\bar{n}$ and k_p at high conversion are in good agreement with the results of this study. This agreement is reasonable since the late stages of a batch emulsion polymerization should correspond to the steady-state conditions of a semicontinuous emulsion polymerization.

Acknowledgment. We thank Rohm and Haas Co. for supporting this research and permitting its publication. We also thank C. J. Neyhart, A. M. Maurice, and T. S. Hackman for significant technical contributions and Professor D. H. Napper for sharing unpublished information.

References and Notes

(1) Ballard, M. J.; Gilbert, R. G.; Napper, D. H.; Pomery, P. J.; O'Donnell, J. H. *Macromolecules* **1984**, *17*, 504.
(2) Ballard, M. J.; Gilbert, R. G.; Napper, D. H.; Pomery, P. J.; O'Sullivan, P. W.; O'Donnell, J. H. *Macromolecules* **1986**, *19*, 1303.
(3) Ballard, M. J.; Gilbert, R. G.; Napper, D. H. *J. Polym. Sci.* **1984**, *22*, 3225.
(4) Mackay, M. H.; Melville, H. W. *Trans. Faraday Soc.* **1949**, *45*, 323.
(5) Bresler, S. E.; Kazbekov, E. M.; Shadrin, V. N. *Makromol. Chem.* **1974**, *175*, 2875.
(6) Schultz, G. V.; Henrici-Olive G.; Olive, S. *Z. Phys. Chem. (Frankfurt/Main)* **1960**, *27*, 1.
(7) Kamachi, M.; Kohno, M.; Kuwae, Y.; Nozakura, S. *Polym. J. (Tokyo)* **1982**, *14*, 749.
(8) For example, the activation energy for the solution polymerization of methyl methacrylate is about 4–6 kcal/mol (Korus, R.; O'Driscoll, K. F. In *Polymer Handbook*, 2nd ed.; Brandrup, J., Immergut, E. H., Eds.; Wiley-Interscience: New York, 1975).

Willie Lau, David G. Westmoreland,* and Ronald W. Novak
Research Laboratories, Rohm and Haas Company
Spring House, Pennsylvania 19477
Received August 25, 1986

Amphiphilic and Polymerizable Porphyrins and Their Copolymerization with Phospholipid: Oriented Fixation of Porphyrins in a Bilayer Membrane

This communication describes the synthesis of novel, amphiphilic and polymerizable porphyrin derivatives (**1**) and their polymers with a polymerizable phospholipid (**2**). **1** had a high compatibility with lipids and formed a stable bilayer membrane with **2**. **1** was copolymerized with **2** in a bilayer state and was covalently and orientedly fixed in a bilayer membrane.

Porphyrins and metalloporphyrins not only are important pigments but also play key roles in biological and biomimetic reaction systems. In these systems much attention has recently been paid to the position and orientation of the porphyrins in matrices: a zinc porphyrin situated in an electron-transfer chain,[1-4] an iron porphyrin as a hemoglobin-like oxygen carrier,[5,6] and a porphyrin fixed in a polymer matrix used for photochemical hole burning.[7,8] In this communication we show that porphyrins can be fixed in a given orientation in a lipid membrane and describe the synthesis of tetraphenylporphyrin derivatives substituted with tetra($\alpha,\alpha,\alpha,\alpha$-alkyl) groups having both a polymerizable double bond and a hydrophilic (carboxylic acid) group at their top position (as shown in **1**). Because not only the hydrophobic–hydrophilic balance but also the stereostructure of **1** are adjusted to a lipid bilayer, it is expected that **1** will form a stable bilayer membrane with a lipid such as **2**, that the polymerizable double bonds of **1** and **2** will be adjacent to each other in a bilayer state, and that in situ copolymerization of **1** with **2** will occur rapidly (Scheme I). Orientation of the porphyrins fixed in the bilayer membrane by the copolymerization was also estimated by electrooptical measurement.

5,10,15,20-Tetrakis($\alpha,\alpha,\alpha,\alpha$-*o*-(8′-(((4″-carboxybutadienyl)carbonyl)oxy)-2′,2′-dimethyloctanamido)phenyl)porphyrin (**1a**) was synthesized by reaction of 5,10,15,20-tetrakis($\alpha,\alpha,\alpha,\alpha$-*o*-(2′,2′-dimethyl-8′-hydroxyoctanamido)phenyl)porphyrin with muconic acid chloride. The structure including the $\alpha,\alpha,\alpha,\alpha$-configuration was confirmed by ^{1}H NMR, ^{13}C NMR, UV–vis, and elemental analysis.[10a] Metal insertion in **1a** gave **1b** and **1c**. 5,10,15,20-Tetrakis($\alpha,\alpha,\alpha,\alpha$-*o*-(20′-(((2″-carboxypropenyl)carbonyl)oxy)-2′,2′-dimethyleicosanamido)phenyl)porphyrin (**1d**) was synthesized by reaction of 5,10,15,20-tetrakis($\alpha,\alpha,\alpha,\alpha$-*o*-(2′,2′-dimethyl-20′-hydroxyeicosanamido)phenyl)porphyrin[5,9] with anhydrous itaconic acid,[10b] and metal insertion gave **1e** and **1f**. **2** was prepared according to the literature.[11]

A bilayer membrane of **1** with **2** was prepared in an aqueous medium through the normal procedure[12] for liposome preparation ([**1**]/[**2**] = 1/(20–50) (molar ratio), [**1**] = 50 μM). **1** was efficiently taken into the **2** bilayer liposome; only 20 mol of **2** was needed to solubilize 1 mol of **1** completely in water. A DSC thermogram of the **2** liposome containing **1** was measured to estimate the phase transition of the bilayer membrane. The **1**/**2** liposome showed an endothermic peak at 18 °C, which was assigned to the gel–liquid crystal phase transition temperature (T_c) of the bilayer membrane and agreed with that for the **2** bilayer liposome itself (18 °C). This suggests that the compatibility of **1** with **2** is large enough to form a stable bilayer membrane.

The bilayer liposome of **2** with **1** was allowed to polymerize under UV irradiation. Complete copolymerization of **2** with **1** was confirmed by UV absorption and ^{13}C NMR spectroscopy: disappearance of absorption bands based on the diene of **1a–c** and **2** or the double bond of **1d–f** and

0024-9297/87/2220-0459$01.50/0